ELSEVIER

S0032-3861(96)00482-X

Polymer Vol. 38 No. 1, pp. 87–98, 1997
Copyright © 1996 Elsevier Science Ltd
Printed in Great Britain. All rights reserved
0032-3861/97/$17.00 + 0.00

Equilibrium concentration profiles of physically end tethered polystyrene molecules at the air–polymer interface

I. Hopkinson, F. T. Kiff and R. W. Richards*
Interdisciplinary Research Centre in Polymer Science and Technology, University of Durham, Durham DH1 3LE, UK

and D. G. Bucknall
ISIS Science Division, Rutherford Appleton Laboratory, Chilton, Didcot, Oxon OX11 0QX, UK

and A. S. Clough
Department of Physics, University of Surrey, Guildford, Surrey GU2 5XH, UK
(Received 16 November 1995; revised 10 February 1996)

Deuteriopolystyrene of molecular weight *ca* 32 000 g mol^{-1} has been functionalized at one end with a fluorocarbon. On mixing this polymer with an unfunctionalized hydrogenous polystyrene a surface excess layer of the deuteriopolymer forms on annealing at 423 K. The surface excess as a function of deuteriopolymer content has been obtained using nuclear reaction analysis and neutron reflectometry, and the shape of the profile from neutron reflectometry alone. From previous secondary ion mass spectral data and by comparison with predictions of surface enrichment theory, it is concluded that the deuteriopolystyrene is tethered by the fluorine label to the air surface. The parameters of this polymer 'brush' obtained experimentally are the surface volume fraction of labelled polymer, the brush height, the surface excess and the layer thickness. The surface excess and surface volume fraction of the deuteriopolymer and the adsorption isotherm (surface excess at a function of equilibrium bulk volume fraction) have been compared to the predictions of a self-consistent field theory. Best agreement is obtained with a sticking energy of $1.9 k_B T$; however, there appear to be some disparities when compared to the limiting 'dry' brush predictions. There is evidence from neutron reflectometry of brush formation *before* annealing of the polymer films. Copyright © 1996 Elsevier Science Ltd.

(Keywords: tethering; surface excess; depth profile; reflectometry)

INTRODUCTION

In a polymer mixture where there are differences in the surface energy of the components it is anticipated that the surface will have a different composition to the bulk of the mixture. The existence of a surface excess of one component is a familiar aspect of mixtures of low molecular weight materials[1]; for polymers some additional factors have to be appreciated. In polymer mixtures the transition from the surface excess region to the bulk composition extends over much longer distances due to the large size of polymer molecules. Typically, this region can have dimensions approaching the radius of gyration of the adsorbing polymer. In addition to the surface energy difference, the interaction between the two polymer components in the bulk needs to be accounted for. Moreover, the maintenance of the composition gradient over the long length scales imposes a considerable free energy penalty on the whole system. Following earlier work by Nakanishi and Pincus[2], Schmidt and Binder[3] provided a detailed thermodynamic description of such surface enrichment, i.e. the surface volume fraction, near surface depth composition profile, etc., using Cahn's square gradient theory and the Flory–Huggins equation for the bulk thermodynamics. This analytical approach was elaborated by Carmesin and Noolandi[4] and expressed in a simplified form which allowed predictions of the surface excess to be made by Jones and Kramer[5]. It is found that, although the surface energy difference is influential in determining the surface volume fraction, ϕ_s, it is the polymer–polymer interaction parameter which plays a major role in determining the shape of the near surface depth profile. Thus, when the system is near the coexistence curve, the surface excess (area under the volume fraction depth profile above bulk volume fraction) is large. A series of experiments on mixtures of hydrogenous and deuterated polystyrene using ion beam analysis and neutron reflectometry have demonstrated that these theoretical descriptions are essentially accurate[6–8]. In this system it has been found that the deuteriopolystyrene enriches the surface of the mixture. Hariharan *et al.*[9] have noted a

* To whom correspondence should be addressed

reversal in this isotopic effect when the molecular weights of the hydrogenous and deuterated polymers are sufficiently different, i.e. when an asymmetric blend is used. Studies of surface enrichment in chemically distinct polymer blends have also been reported[10–13] where techniques such as attenuated total reflectance (ATR) i.r. absorbance, secondary ion mass spectrometry (SIMS) and X-ray photoelectron spectroscopy (X.p.s.) as well as neutron reflectometry have been used.

In the description of a surface enriched layer outlined above, it is assumed that each segment in the adsorbing molecule has equal 'sticking energy' to the surface. Another aspect of interest is the attachment of a polymer chain by one end to a surface. In this situation the adsorbed layer is described as a brush. The spatial extent of the brush (i.e. its height) is determined by the molecular weight of the adsorbing molecule, the molecular weight of the matrix and the density of adsorbing ends per unit area at the interface (areal density). There are two extreme cases. A 'wet' brush where the matrix molecular weight is considerably less than the adsorbed polymers and there is a high concentration of these matrix molecules in the brush. As the molecular weight of the matrix increases, its volume fraction within the brush decreases until a point where there is no further change on increasing the molecular weight. The system is now at the other extreme, the 'dry' brush. Much of the attention thus far has been focused on wet brush systems. These have evident applications in the steric stabilization of colloidal dispersions and an encyclopaedic discussion of wet brush theory and experiment has recently appeared[14].

Theoretical descriptions of end attached polymers fall into two broad groups: scaling theories and self-consistent field (SCF) theories; the majority of both of these approaches have been concerned with wet brushes. Scaling theories generally produce equations relating the brush height to the areal density of the adsorbed chains, but say nothing about the concentration profile of polymer normal to the surface. Perhaps the best known SCF theory for wet brushes is that of Scheutjens and Fleer[15], and specific SCF solutions for dry brushes have been obtained in the special case of the segment density distribution within the microphase separated regions of block copolymers[16]. Shull[17] has produced numerical solutions to the SCF calculation for end absorbed polymers, which can be examined experimentally using such parameters as the surface volume fraction, surface excess (z^*) and by obtaining the near surface depth profile. Experimental studies of the near surface depth concentration profile of polymers have been reported for the case of a polymer attached to a solid surface. Clarke and co-workers[18–20] have discussed the influence of the matrix polymer on the near surface depth profile and also discussed the kinetics of formation of the equilibrium layer. Mansfield *et al.*[21] have used neutron reflectometry to obtain depth profiles for polystyrene end attached to silicon at the silicon–cyclohexane interface. In all of these studies one end was functionalized with a group which was adsorbed to the solid substrate surface. In an earlier paper[22], we reported the results of a SIMS and X.p.s. investigation of mixtures of a fluorine single end labelled deuteriopolystyrene (DPSF) with hydrogenous polystyrene (HPS). For relatively low molecular weights of the two polymers ($\sim$40 000 g mol^{-1}) and in the absence of end labelling, no evidence of enrichment of the surface by the deuteriopolystyrene was observed. This finding was entirely in agreement with the predictions of mean field theory since the system was in the one phase region and very distant from the coexistence curve. When the deuteriopolystyrene was labelled at one end by the low surface energy tridecafluoro-1,1,2,2-tetrahydrooctyl-1-dimethylsilyl residue, the presence of both fluorine and deuterium atoms at the surface at concentrations in excess of the average bulk value was detected, which indicated that the deuteriopolymer was becoming attached to the air–polymer interface. We discuss here the results of ion beam analysis and neutron reflectometry studies on thin films of these mixtures. We have obtained the near surface depth profile of the DPSF as a function of the DPSF content of the films from neutron reflectometry, and from these data the surface volume fraction and surface excess have been obtained. The analysis of the neutron reflectometry data has been performed using three functional forms and a maximum entropy method, where the latter involves no *a priori* assumptions about the nature of the near surface depth profile. A comparison of these fitting methods is made. Nuclear reaction analysis data on the same DPSF/HPS mixtures has provided values for the surface excess, which have been compared to those obtained by neutron reflectometry. Finally, the near surface depth profiles have been compared to the predictions of a SCF calculation where the only adjustable parameter is the sticking energy of the funtionalized end. A qualitative method of estimating this sticking energy from available data is also set out.

THEORY

Self-consistent field calculations

Only a descriptive overview of the procedure used is given here, as a full derivation is available in the original paper by Shull[17]. Our aims are to identify the important parameters which describe quantitatively the near surface depth profile. We consider a two-component mixture of polymer 1 and polymer 2, where polymer 1 has no surface active end, but polymer 2 has one end which has a surface interaction energy of $k_B T \chi_c^S$. This labelled end has an interaction with the bulk of the polymer mixture of $k_B T \chi_c^B$, which differs from the Flory–Huggins interaction parameter χ between segments of polymers 1 and 2 which are not surface active. This polymer mixture is placed in contact with an impenetrable surface at a distance $z = 0$; normal to this surface a lattice is created the side length of each lattice cell being a, the statistical segment size. The surface active ends which are absorbed at the surface are confined to a layer of size $\delta_s (= a)$ adjacent to the surface, and the configuration of the polymer normal to the surface is discussed in terms of a set of distribution functions. Each distribution function must relate to a segment sequence which must contain an end segment, either of the surface inert polymer 1 or the surface active end of polymer 2 or the surface inert end of polymer 2. These distribution functions are related by a series of recursion relations which are weighted by the appropriate mean field for the segments concerned. The mean field is calculated from the Flory–Huggins expression for the free energy change on mixing. Calculation of the volume fraction of the end

tethered molecule in any layer, i, normal to the surface is made from the product of the two distributions at i of polymer 2 which start from the labelled end and from the inert end. Conversion of this product to a volume fraction is made via the proportionality factor $\exp(\mu_2/k_BT)$, where μ_2 is the chemical potential of polymer 2 chains and includes contributions from the surface active end and a term describing the change in mean field with layer number. (This corresponds to the squared gradient term introduced by Cahn[23] and used by Schmidt and Binder[3].) At sufficiently large depths, z, into the polymer mixture this gradient term must be zero. In applying the solution, a chemical potential distribution is initially guessed and the configuration of polymer 2 normal to the interface is calculated. The chemical potential is recalculated and the new configuration resulting from any change is obtained. This process is reiterated until a configuration consistent with the chemical potential distribution is obtained.

A normalized near surface depth profile is obtained, i.e. the volume fraction of the tethered chain as a function of z/R_{g2}, where R_{g2} is the radius of gyration of the end tethered polymer. This normalized profile is determined by the normalized surface excess, z^*/R_{g2} and the ratio of the degrees of polymerization of the two polymers, N_1/N_2, where the surface excess is defined by

$$z^* = \int_0^\infty (\phi_2(z) - \phi_2(\infty))\mathrm{d}z \qquad (1)$$

The 'sticking energy' of the end group is given by $k_BT\beta$ where

$$\beta = \chi_e^B - \chi_e^s + 1.1\ln(\delta_s/R_{g2}) \qquad (2)$$

The χ_e^s term as well as accounting for interactions between the chain end and surface also includes any local entropic effects. The confinement of the adsorbed chain end to a region of thickness δ_s contributes to these local entropic effects and, because of chain continuity, this restriction also adds a non-local contribution to the confinement entropy, which is the natural logarithm term in equation (2). When β is positive there is a net thermodynamic driving force for adsorption of the molecule at the surface. A characteristic behaviour of the variation of z^*/R_{g2} with equilibrium bulk fraction as β varies has been noted[17].

Neutron reflectometry (NR)

The fundamental principles and applications of neutron reflectometry have been set out in a number of publications[24–26]. A description of the technique is given here without the derivation of any equations; however, we focus some attention on the analysis of reflectometry data so that artefact free values of parameters to compare with SCF predictions are obtained.

When a neutron beam is incident on a smooth surface at any angle greater than the critical angle, part of the beam is specularly reflected from the surface and part of the beam undergoes refraction into the specimen. If the neutron refractive index of the material normal to the surface is a quantity varying with depth, then the refracted beam will be specularly reflected in a manner determined by this neutron refractive index variation. This results in a dependence of the intensity of specular reflection on the incident angle of the beam. Experimentally, rather than using the grazing incidence angle θ, the scattering vector normal to the surface, is used. This quantity, symbolized by Q, is defined as

$$Q = (4\pi/\lambda)\sin\theta \qquad (3)$$

(where λ is the wavelength of the neutron) and we discuss the specular reflection in terms of the reflectivity $R(Q)$ as a function of Q, where $R(Q)$ is the ratio of the reflected intensity to the incident intensity. Since absorption effects can usually be ignored in neutron reflectometry from polymers, the neutron refractive index at any point in the specimen is determined by the scattering length density at that point. The scattering length density is controlled by the volume fraction composition of the specimen at the depth probed. Consequently, the reflectivity profile [$R(Q)$ as a function of Q] contains within it all the information on the near surface composition depth profile of the specimen. Evidently, the molecule of interest in this composition profile needs to be contrasted with the matrix in which it is mixed. For neutron reflectometry from polymers this contrast can be achieved by deuterating the molecule; however, due care should be taken that this deuteration does not introduce significant alterations in the bulk thermodynamic and surface behaviour.

Ideally, the scattering length density profile (and hence the composition profile) could be obtained by Fourier inversion of the reflectivity profile. However, the limited Q range available and the loss of phase information inherent in such a procedure makes direct inversion impracticable. Various methods of analysis of reflectivity profiles have been discussed[27–30]; in the main there are two approaches. In the first the specimen is divided into a number of layers of defined thickness and composition, and the reflectivity of this lamella stack is calculated by the exact optical matrix methods and compared by a least squares method to the experimental reflectivity. We have used a maximum entropy[31] variant of this method here. A defined number of lamella elements are used to describe the *total* thickness of the sample. In our case we have used 150 layers of fixed thickness with the composition of each layer allowed to vary during the fitting process to the experimental data. This functional form free fitting procedure has attractions in that no *a priori* model is imposed and any possible concerns about the uniqueness of the eventual solution are minimized. The second method used is to apply a functional form to describe the concentration profile and optimize the parameters by non-linear least squares fitting (or some equivalent procedure, e.g. simulated annealing[32]) to the experimental reflectivity. In such a procedure, questions about the uniqueness of the model should always be borne in mind and where possible the model should be validated by other information if available and other functional forms should also be used. We have used three functional forms in the work reported here.

Although the free form model *appears* to be the most practical procedure to adopt, it can produce artefacts. These arise from the finite Q range, which produces oscillations in the volume fraction profile. The oscillations can be reduced by applying a Gaussian smoothing function. More perturbing is the inability of the maximum entropy method to deal with the sharp reduction in concentration at the transition from polymer film to air.

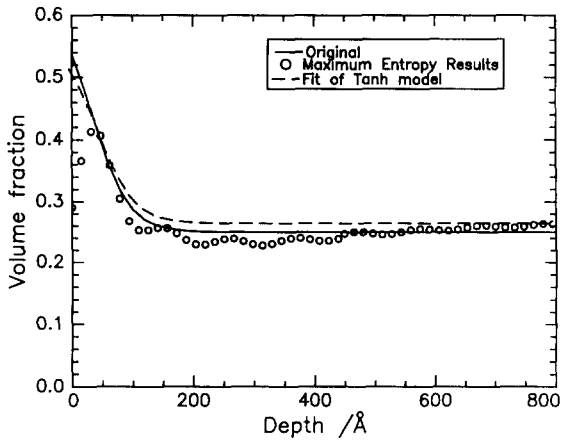

Figure 1 Volume fraction profiles obtained by fitting a simulated reflectivity profile generated by an optical matrix calculation and equation (4): (—) original near surface depth profile; (O) volume fraction profile obtained using free form maximum entropy fitting to neutron reflectometry profile; (- -) volume fraction profile obtained by non-linear least squares fitting of neutron reflectometry profile using the functional form of equation (4)

In an attempt to reduce the entropy penalty associated with such a sharp reduction, the maximum entropy method attempts to place a smooth decrease in concentration of the surface species near the surface. This leads to a sharp downturn in the volume fraction profile at the surface. To quantify these effects we generated a model volume fraction profile using the functional form:

$$\phi(z) = \phi_B + \left(\frac{\phi_s - \phi_B}{2}\right)\left[1 + \tanh\left(\frac{2(z_{off} - z)}{w}\right)\right] \quad (4)$$

for DPSF in HPS. Equation (4) is the analytical form which best describes the near surface depth profiles obtained by SCF theory. In equation (4), z_{off} is the brush 'height' and w the brush width parameter, i.e. width of the overlap region between brush and matrix at $\phi_s = 0.5$. A total film thickness of 4000 Å was used together with $\phi_s = 0.63, \phi_B = 0.25, z_{off} = 33.5$ and $w = 120$. Reflectivity profiles were calculated for this arrangement by the exact optical matrix method incorporating instrument resolution effects and a mean square roughness of 25 Å^2 at the air–polymer and polymer–substrate (silicon; see below) interfaces. The reflectivity so obtained was then analysed by both free form fitting and functional form methods. The results are compared with the original volume fraction profile in *Figure 1*. The oscillations and sharp reduction are evident in the free form model whereas the functional form fit recovers the initial volume fraction profile reasonably well. Notwithstanding these cautionary remarks, NR is capable of providing near surface depth profiles at length scale resolutions of 10–20 Å and for a sample thickness up to *ca* 5000 Å.

Nuclear reaction analysis (NRA)

Like NR, NRA applied to polymers relies on using deuterated polymers as a probe of the concentration profile[33,34]. In NRA, polymer samples containing deuterated polymer are bombarded with $^3He^+$. These ions undergo a nuclear reaction with deuterium nuclei (deuterons):

$$^3He^- + ^2H \rightarrow ^4He + ^1H^+ + \text{Energy}(18.35\,\text{MeV})$$

As the $^3He^+$ penetrate deeper into the sample they lose energy. They are thus less able to propel deuterons forward, and protons ejected at backward angles will have a higher energy the greater the depth into the sample from which they originated. Consequently, the energy spectrum of the ejected protons constitutes a composition 'map' of the location of deuterium in the specimen when the known stopping powers of $^3He^+$ in the polymer are used in conjunction with an absolute energy scale. NRA is able to analyse samples up to several micrometres thick, but the length scale resolution is much less than with NR; a quoted best resolution length scale is *ca* 150 Å[34]. The advantage of NRA lies in the fact that no inversion procedure or application of a model is required to obtain composition depth profiles. Profiles are obtained directly from the proton energy spectrum by comparison with a spectrum from a uniformly deuterated sample and only incorporates the resolution function of the instrumentation.

Table 1 Molecular weight and molecular weight distribution of hydrogenous and end labelled deuterated polystyrenes

Polymer	M_w (10^3 g mol^{-1})	M_w/M_n
DPSF	31.7	1.1
HPS	44.7	1.1

EXPERIMENTAL

Polymers

Both HPS and DPSF polymers were prepared by anionic polymerization at room temperature under high vacuum. In each case, benzene was used as the solvent and secbutyl-lithium was the initiator. The living HPS was terminated by adding degassed methanol. For the deuteriopolystyrene, an excess of tridecafluoro-1,1,2,2-tetrahydroctyl-1-dimethylchlorosilane [Cl-Si$(CH_3)_2(CH_2)_2(CF_2)_5CF_3$] was added. The polymers were isolated by precipitation in methanol and subsequent drying at 353 K *in vacuo*. To ensure complete removal of any fluorine containing low molecular weight contaminants, the DPSF was dissolved and reprecipitated three times. Separate experiments on HPS 'spiked' with the fluorosilane had shown that this procedure was successful in its removal to levels at which it could not be detected by ^{19}F n.m.r. *Table 1* shows the average molecular weights of the HPS and DPSF polymers obtained by size exclusion chromatography using both tetrahydrofuran (THF) and chloroform as solvents. For the THF system, both refractive index and viscosity detection were used. Only refractive index detection with polystyrene calibration was used for the chloroform system.

Thin film preparation

Thin films of mixtures of DPSF with HPS for NR were prepared by spinning 7% (w/v) solutions in toluene on to the polished surface of cylindrical silicon blocks. The silicon blocks had a diameter of 50 mm and were 5 mm thick and were used without removing the natural silicon

Table 2 Parameters obtained using tanh profile to fit neutron reflectometry data

Volume fraction DPSF (ϕ_B)	Unannealed					Annealed				
	ϕ_s	z_{off} (Å)	w (Å)	z^* (Å)	Norm. χ^2	ϕ_s	z_{off} (Å)	w (Å)	z^* (Å)	Norm. χ^2
0.02_7	0.18 ± 0.02	25 ± 2	50 ± 4	4 ± 1	10.5	0.11 ± 0.02	56 ± 2	54 ± 4	4.7 ± 1	7.6
0.08	—	—	—	—	—	0.34 ± 0.04	68 ± 2	65 ± 4	17 ± 1	4.2
0.11	—	—	—	—	—	0.46 ± 0.04	55 ± 2	112 ± 6	21 ± 1	7.6
0.14	—	—	—	—	—	0.57 ± 0.05	64 ± 2	78 ± 6	28 ± 2	5.5
0.18	0.43 ± 0.04	40 ± 2	71 ± 6	13 ± 1	5.6	0.54 ± 0.05	72 ± 2	127 ± 6	30 ± 2	3.4
0.29	0.59 ± 0.05	54 ± 2	41 ± 4	17 ± 1	5.3	—	—	—	—	—
0.28	—	—	—	—	—	0.77 ± 0.05	78 ± 2	104 ± 6	40 ± 2	5.3
0.45	0.62 ± 0.05	65 ± 2	66 ± 6	12 ± 1	4.1	0.73 ± 0.05	90 ± 3	93 ± 6	26 ± 2	3.3

Norm. χ^2 is the value of normalized χ^2 returned from the fit to the reflectometry data

oxide layer, but were cleaned by ultrasonication in toluene. A spinning speed of 2000 rev min^{-1} was used and after the film had formed the specimens were annealed at 423 K for two days under vacuum. Unannealed specimens were also prepared and retained for a few selected mixtures of DPSF in HPS. Contact profilometry was used to determine the thickness of each film, average thicknesses were *ca* 4000 + 200 Å. Such thick films had two advantages. Firstly, the contribution of the silicon oxide layer (~ 15 Å thick) to the reflectivity profile is negligible. Secondly, de-wetting of these low molecular weight polymer films on annealing is prevented. A disadvantage is the absence of any characteristic Kiessig fringes due to the total thickness of the film; consequently, we had to rely on profilometry data for these values. Several films were prepared covering a DPSF volume fraction range from *ca* 0.05 to 0.5. Thin films for NRA were prepared in a similar manner, but thinner silicon wafers (~ 0.5 mm thick) were used since NRA is not sensitive to distortions of the substrate which may result on annealing at elevated temperatures.

Neutron reflectometry

NR profiles on the thin films were obtained using the CRISP reflectometer on the UK pulsed neutron source ISIS at the Rutherford Appleton Laboratory. A Q range from 0.01 to 0.06 Å^{-1} was used, which necessitated the use of two different incident angles of 0.25 and 0.6°. Collimating slit widths were adjusted in the range 2–4 mm to maintain the same geometric resolution ($\Delta Q/Q$) for each incident angle used. Data from the lowest Q range were placed on an absolute scale by setting the reflectivity below the critical Q value to 1. Each of the data sets was then scaled to these data and all three sets combined to give a single reflectometry profile. A position sensitive multidetector was used to detect the specularly reflected beam. This detector allowed us to estimate and subtract the background under the specular peak at each value of Q. All reflectivities given here are background subtracted and on an absolute scale.

Nuclear reaction analysis

NRA experiments were performed at the EPSRC device fabrication facility at the University of Surrey, Guildford, UK. A $^3He^+$ beam energy of 0.7 MeV was used to bombard a sample oriented at 15° to the incident beam, and ejected protons were detected at an angle of 165° to the incident beam direction, i.e. backward detection was used. The raw data of counts *versus* channel number were converted into an energy spectrum and subsequently volume fraction profiles, using available software, the energy calibration data for the silicon surface barrier detector and a comparison spectrum from a sample of 1 μm thick film of deuteriopolystyrene.

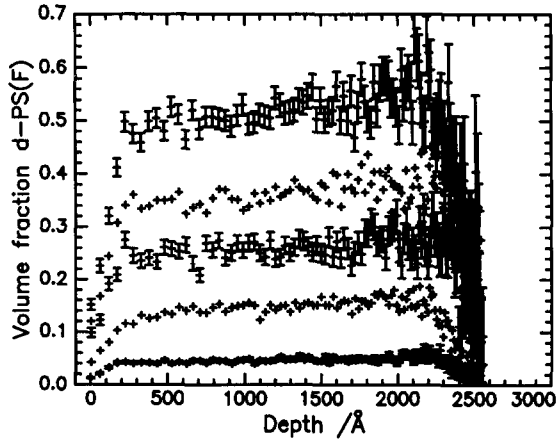

Figure 2 Volume fraction profiles obtained from nuclear reaction analysis on unannealed films. Data have not been deconvoluted from the resolution function. Nominal bulk volume fractions: 0.5; 0.35; 0.25; 0.15; 0.05 of DPSF in descending order

RESULTS

Nuclear reaction analysis

Figure 2 shows the volume fraction profiles obtained for the unannealed DPSF/HPS films, and the volume fractions in the plateau region agree well with the average volume fraction of the mixture used. These data indicate that, within the resolution of the instrument used, there is no detectable adsorption of the DPSF to the vacuum (or air) surface (depth = 0 Å) before annealing. The apparent thickness of the film of 2500 Å is considerably less than the 4000 Å measured by profilometry. This is due to the $^3He^+$ being stopped before reaching the polymer–silicon interface due to the long pathlength consequent on the glancing incident angle of 15° of the beam on the sample. After annealing for two days, the

Table 3 Surface excess of DPSF obtained from NRA data

Bulk volume fraction	z^*(Å)
0.04	13
0.14	27
0.21	30
0.33	56
0.48	32

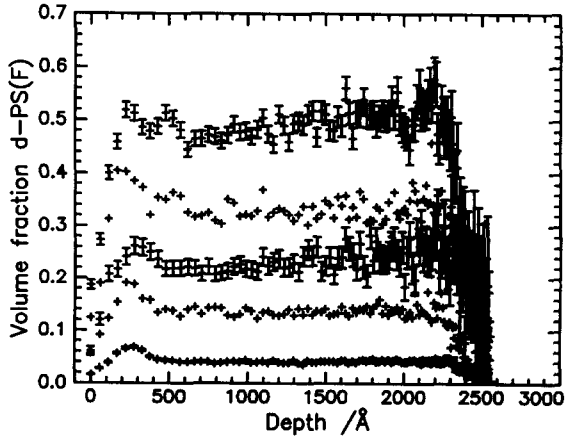

Figure 3 Volume fraction profiles (undeconvoluted) obtained by nuclear reaction analysis on annealed films. Order of data as in *Figure 2*

NRA data reveal a small surface excess of DPSF in the films (*Figure 3*). The data in both *Figures 2* and *3* are convoluted with the resolution function of the instrument and we discuss this later.

Neutron reflectometry

NR profiles obtained before and after annealing are shown in *Figure 4* as $Q^4R(Q)$ plots, where the increase in reflectivity on annealing is evidence that the deuteriopolymer has a higher concentration near the surface. In an attempt to compare fitting functional forms and the possible incorporation of artefacts, four methods have been used to fit the neutron reflectivity data. Firstly, the widely used error function profile:

$$\phi(z) = \frac{\phi_S - \phi_B}{2}\left[1 + \mathrm{erf}\left(\frac{z_{off} - z}{w}\right)\right] + \phi_B \qquad (5)$$

Secondly, the functional form of equation (4) was used; thirdly a 'stretched' exponential of the form:

$$\phi(z) = (\phi_S - \phi_B)\exp[-(z/\xi)^{\beta}] + \phi_\infty \qquad (6)$$

where β along with ϕ_0, ϕ_∞ and ξ were fitting parameters. Lastly, the maximum entropy method developed by Sivia *et al.*[31] and partially discussed earlier was applied. Representative fits using equations (4) and (5) and the maximum entropy method are shown in *Figure 5*. The stretched exponential always returned a value of β very close to 2.0, and the fits were essentially identical to the tanh functional form fits. In each of these fits the presence of the silicon oxide layer and roughness at the air–polymer and polymer–substrate interface was included as was the instrumental resolution. Furthermore, we also incorporated the possibility of the existence of the immediate surface layer containing the fluorosilyl residue. If the dimensions and scattering length

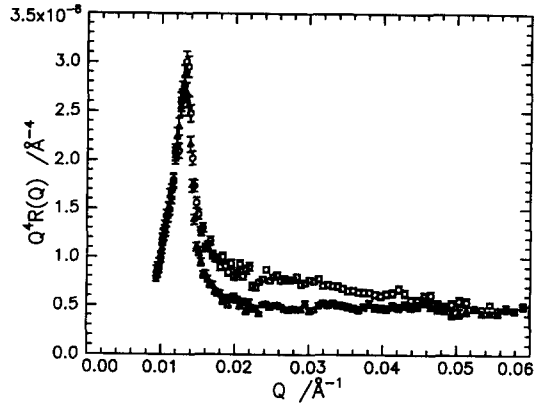

Figure 4 Neutron reflectometry data as $Q^4R(Q)$ for unannealed and annealed polymer films. Bulk volume fraction of DPSF is 0.5. (○) Annealed; (△) unannealed

density were fixed at those approximating to those for this end group (*ca* 20 Å and 2.72×10^{-6} Å^{-2}, respectively), then the fitted curves were always below the measured reflectometry for $Q \geq 0.045$ Å^{-1}. Allowing these parameters to be fitting variables resulted in a layer thickness of *ca* 5 Å and a scattering length density approaching that of air being returned and with a negligible effect on the parameters pertaining to the volume fraction profile of the deuteriopolystyrene portion. The maximum entropy fitting process overestimates the position of the critical edge for the 0.5 DPSF volume fraction polymer, but gives an acceptable fit to the data for Q greater than *ca* 0.014 Å^{-1}. For the mixture containing a DPSF volume fraction of 0.05, although the critical edge was well reproduced, data at higher Q values were underestimated. Consequently, for the higher volume fractions of DPSF the bulk volume fraction will be overestimated by the maximum entropy method whereas for the lower volume fractions the air surface volume fraction will be underestimated. By contrast the use of equation (4) as a functional form reproduces the critical edge well and also fits reasonably well to the data at higher Q for the lower volume fractions of DPSF, but is consistently low at higher Q for the mixture containing 0.5 volume fraction of DPSF. The error function gives acceptable fits to both critical edge and the data at the higher Q values.

Figure 6 shows the volume fraction profiles obtained from the fitting procedures using equations (4) and (5) and the maximum entropy fits. [The volume fraction profile from the stretched exponential was identical to that of equation (4)]. The error function profile results in a lower surface volume fraction than the tanh profile, but extends further into the bulk of the polymer film, as a result the surface excess values calculated from the two profiles are within 4 Å of each other. The maximum entropy profiles generally lie in between the tanh and error function profiles, except for the very lowest DPSF volume fraction profile investigated; furthermore, the bulk volume fraction obtained is marginally higher than that given by the functional form fits. However, the maximum entropy obtained volume fraction profiles have a sharp decrease in volume fraction as the polymer surface is approached. For comparison with the SCF theory of Shull[17], values of ϕ_B, ϕ_S and z^* have been calculated using equation (4). These values are given in *Table 2*, together with values obtained for

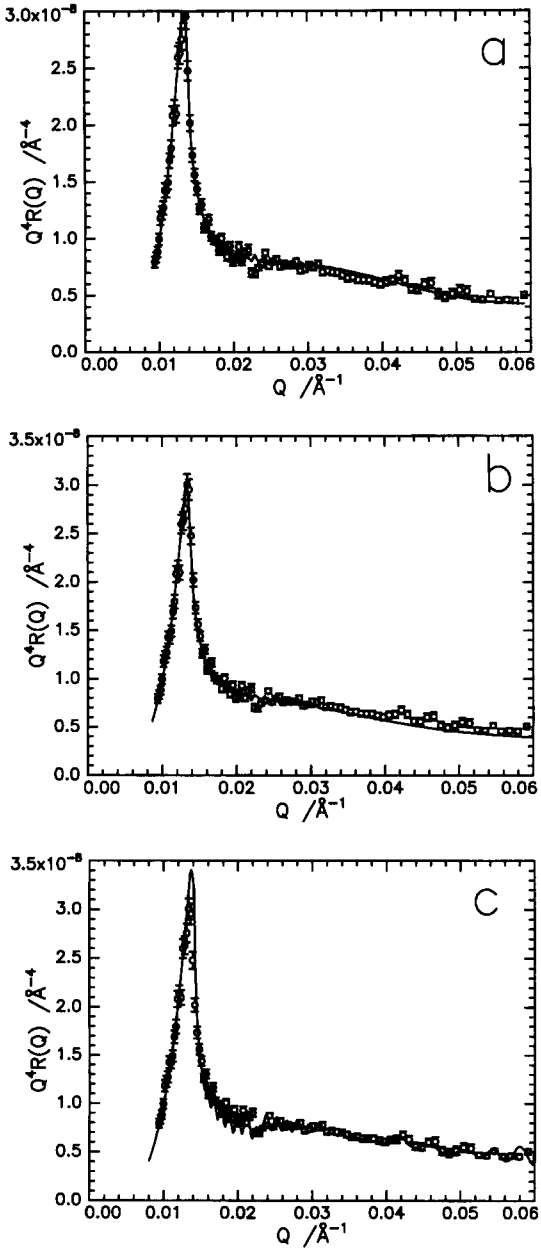

Figure 5 (a) Fit (solid line) of reflectivity calculated using error function expression [equation (5)] to reflectivity data; (b) fit (solid line) of reflectivity using tanh expression [equation (4)] to reflectivity data; (c) maximum entropy analysis fit to reflectivity data. For all cases the data pertain to the annealed sample with a DPSF bulk volume fraction of 0.5

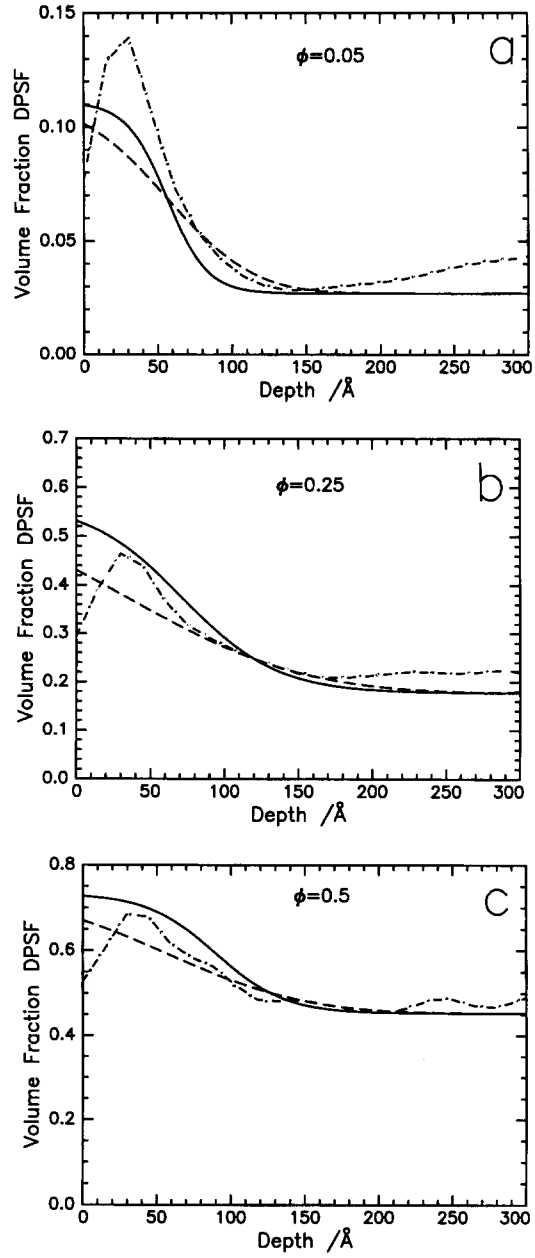

Figure 6 Volume fraction profiles obtained for annealed films by maximum entropy and functional form methods. Solid lines — tanh functional form fits; - - - error function fits; ····· maximum entropy fits. (a) Bulk volume fraction 0.027; (b) bulk volume fraction 0.18; (c) bulk volume fraction 0.45

the unannealed films and the normalized χ^2 values for the fits to the NR data. Values of the surface excess, z^*, were calculated using equation (1) between the limits of $z = 0$ and $z = \infty$ (effectively the total thickness of the film). A notable feature of *Table 2* is that the DPSF is partially adsorbed in the unannealed films. A surface excess of DPSF in the unannealed blends was also evident in the volume fraction profiles obtained by all methods of analysis of the reflectometry data. Hence, we do not believe that the surface excess observed before annealing is an artefact of the use of a functional form for the volume fraction profile normal to the surface.

DISCUSSION

Although NR gives a small surface excess in the unannealed films no such excess is evident in the NRA data on similar samples and consequently since there are no observable features in these NRA profiles we have not attempted to fit these profiles using functional forms where an excess surface layer is explicitly included. All we can say about these data is that they give an overall volume fraction of DPSF which is in agreement with the composition of the DPSF/HPS mixture used. We remarked earlier that, after annealing, a small surface excess became apparent in the NRA profiles on the DPSF/HPS mixtures. We have attempted to extract

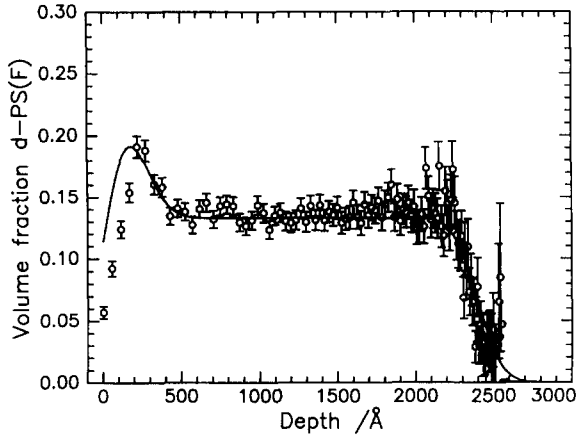

Figure 7 Fit of a simple two-block model calculated with a Gaussian resolution function to the nuclear reaction analysis data

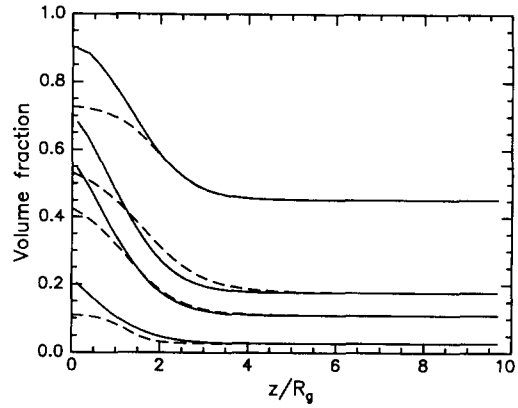

Figure 9 Comparison of near surface depth volume fraction profiles calculated by self-consistent field theory model (- - -) with those obtained from neutron reflectometry using the tanh functional form. Bulk volume fractions in descending order

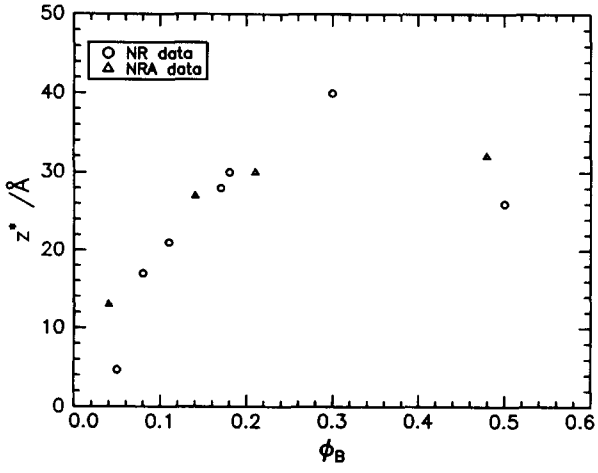

Figure 8 Surface excess, z^*, as a function of equilibrium bulk volume fraction: (O) neutron reflectometry data; (Δ) nuclear reaction analysis data

physical parameters which characterize the surface excess from these data in two ways. Firstly, we have taken the functional form of equation (4) and convoluted this with an instrumental Gaussian resolution function. This convoluted function has then been non-linearly least squares fitted to the data. Secondly, in consideration of the poor spatial resolution of the NRA instrument used, a simple two-block structure was convoluted with the Gaussian resolution and fitted to the data. The two-block structure consisted of a tall thin rectangular area on top of a second short wide rectangle. The latter representing the bulk region and the former the surface excess region of the thin film. In common with Clarke *et al.*[19] (who had much larger surface excesses in their system) we found that the fit was insensitive to the parameters of the near surface depth profile [z_{off} and w in equation (4), height and width of the surface box in the simple model] as long as the excess area under the profile was unaltered. The surface excess, z^*, obtained from the NRA data is unaffected by the resolution in those cases where a surface excess is observable. Consequently, we only report the surface excess values, z^*, in *Table 3* because we can say nothing with certainty about the shape of the near surface depth profile from these data.

Additionally, the fits to the NRA data, typified by *Figure 7*, were not successful in fitting to the leading edge of the NRA profiles and hence the z^* values should be viewed cautiously. The major aspect to be drawn from these data is that they are direct evidence of a surface excess layer being formed after annealing. Values of the surface excess as a function of bulk volume fraction obtained from NR and NRA are shown in *Figure 8*.

Before proceeding further with a detailed comparison of our data with SCF theory, it is appropriate that we should confirm that the DPSF is indeed attached by its end to the air surface. The volume fraction profile for the combination of deuteriopolystyrene and HPS (i.e. in the absence of the fluoro end label) calculated using the simplified relations of Binder[3,5] and the values of χ[35] and $\Delta\gamma$[7] (the surface energy difference) for mixtures of H and D polystyrene shows no surface enrichment and this has been confirmed by our earlier SIMS experiments on similar mixtures of H and polystyrenes where no excess of D polymer was observed. Additionally, separate NR experiments on D polystyrene and H polystyrene mixtures where no fluorine labelling was used have shown that no surface excess layer of deuteriopolymer is observable[36]. The fluorine end label clearly brings about a surface excess of the deuteriopolymer at the surface and, since X.p.s. results have indicated an excess of fluorine[22,37] at the surface, it seems reasonable to conclude that the DPSF is end tethered at the air surface, and we have attempted to compare the volume fraction profiles obtained from the NR data with the predictions of Shull's SCF theory[17].

To speed computation, the true values of the degree of polymerization have not been used, but the ratio of HPS to DPSF has been preserved; thus, for HPS a degree of polymerization of 160 was used whilst for DPSF a value of 100 was used. Because of this we compare the output from the calculations and the results of experiment via normalized parameters. In the calculations the depth from the surface is the dimensionless parameter z/R_g and we obtain the normalized surface excess, z^*/R_g, where R_g is the radius of gyration of the end tethered molecule. For DPSF we have used the unperturbed radius of gyration of polystyrene of equivalent molecular weight obtained from the literature[38,39]; a value of 46 Å was used here. For the Flory Huggins interaction parameter required in the

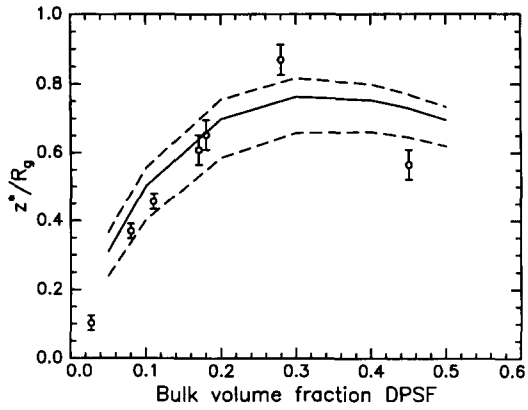

Figure 10 Adsorption isotherm at the air surface of DPSF in HPS. The solid line is calculated from self-consistent field theory with a sticking energy of $1.9k_BT$. The dashed lines are the adsorption isotherms calculated for sticking energies of $1.7k_BT$ (lower) and $2.1k_BT$ (upper)

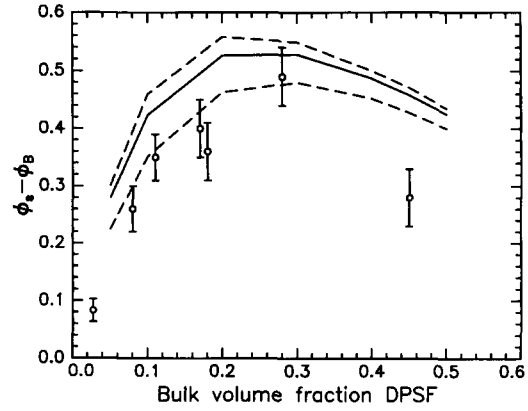

Figure 11 Difference in surface volume fraction and bulk equilibrium volume fraction of DPSF as a function of bulk equilibrium volume fraction. Solid and dashed lines are self-consistent field predictions as in *Figure 10*

calculation, we used a value of χ such that the value of χN in the SCF calculation was equal to χN in the experimental system, where in each case the value of N used was the geometric mean of the two slightly different degrees of polymerization of the HPS and DPSF used. The molecular weights of the two polymers used here were sufficiently low such that $\chi N \simeq 0$ and so we set $\chi = 0$. Given that the equilibrium bulk fraction is known for each blend, the only adjustable parameter is the surface free energy difference or sticking energy term, β. Repeated SCF calculations have been performed adjusting β until the best agreement between computed and surface excess values was obtained. Using the normalized surface excess as a criterion of validity we found that acceptable agreement with measured normalized surface excess values could be obtained using a single value of the sticking energy of $1.9k_BT$ for all compositions of DPSF and HPS used. However, the detailed agreement between experiment and theory is not good, especially for the extremes of the DPSF concentration range used (*Figure 9*). If the criterion of agreement between measured and theoretical profiles is taken to be the surface volume fraction, then the normalized surface excess values obtained from the theoretical volume fraction profiles are much smaller than those obtained experimentally. Moreover, the calculated profiles in the surface excess region are considerably smaller in value than those measured.

In *Figure 10* we compare the adsorption isotherms (as z^*/R_g as a function of ϕ_B) from the experimental data and the theoretical profiles. The sensitivity of the SCF calculations to the value of β is illustrated by the lines calculated for $\beta = 1.9 \pm 0.2k_BT$ included in *Figure 10*. However, the apparent agreement between experiment and theory implied by this figure is not evident in the profiles of *Figure 9*. The difference becomes more apparent in *Figure 11* where $(\phi_S - \phi_B)$ values are plotted as a function of ϕ_B; evidently the SCF theory overestimates the immediate surface volume fraction of DPSF. The SCF theory assumes that adsorption is restricted to the first lattice layer below the surface whereas there is probably some adsorption due to interactions at longer distances from the first lattice layer. In addition to reducing the immediate surface volume fraction at the surface, such longer range adsorption would also lead to the 'flattening' of the volume fraction profiles. The comparisons shown in *Figure 9* are consistent with the weak adsorption implied in the value of β obtained, suggesting that the areal density of fluorine ends at the surface is low. Excellent agreement with SCF predictions has been obtained by Clarke *et al.*[18] where D polystyrene grafted to the silicon surface had been overcoated by H polystyrene and then annealed. For these cases the SCF profiles were slightly broader than those measured. A notable feature of these data was the good agreement obtained with theory even when the matrix polymer had a molecular weight an order of magnitude smaller than the grafted polymer, although the SCF theory states that the ratio of molecular weights should be greater than or equal to 1.

This naturally leads to the question of the validity of the application of the SCF theory to our data where weak adsorption is evident and notwithstanding the good agreement of the extent of the measured surface excess with that predicted as evident in *Figure 10*. We note that Shull[17] states that the profiles obtained for the strong adsorption case can be applied to weak adsorption provided that the surface volume fraction of the adsorbing polymer is less than 0.8 and that χN is very small. This latter condition is certainly fulfilled and the surface volume fraction requirements are met by all the mixtures we investigated, but we do approach the limiting criterion for the higher concentration limits. The comparison between measured and theoretical profiles is rather similar to that observed by Jones *et al.*[8] for DPS absorbed at the silicon substrate surface, although their volume fraction profiles had maxima close to the silicon surface, which was accounted for by the difference in interaction energy for H and D segments with the silicon surface. The low areal density of the organosilane end groups of the DPS at the silicon surface meant that much of the air–polymer interaction was due to contacts between the air and the segments of the two polymers, hence the need to account for the difference in interaction energies.

Other differences from the predictions of the SCF theory became apparent when compared to predictions for the limiting dry brush case. Shull[17] remarks that the

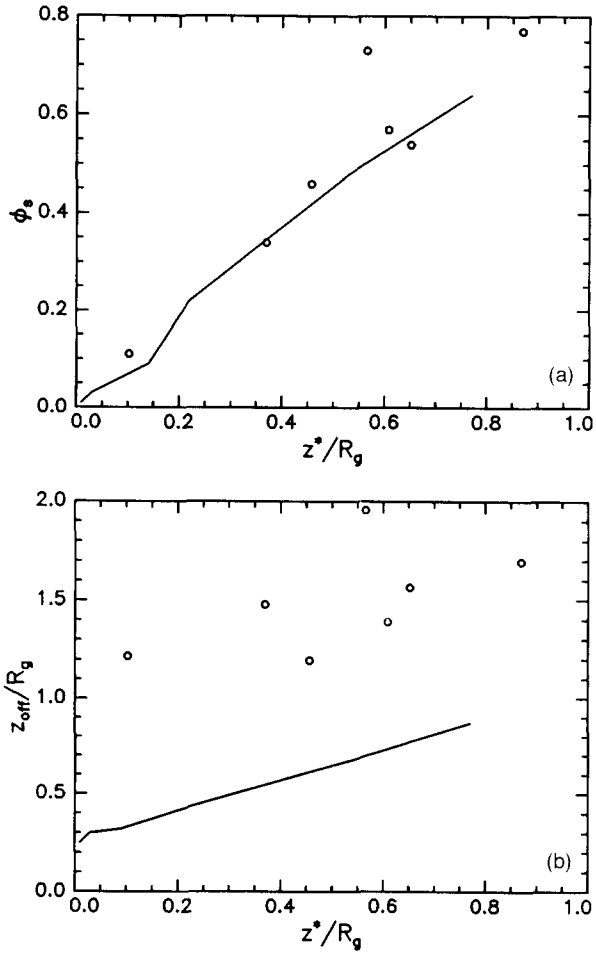

Figure 12 Comparison of experimentally obtained parameters for DPSF/HPS mixtures to values calculated from self-consistent field model in the limiting dry brush case: (a) surface volume fraction as a function of normalized surface excess; (b) normalized brush height as a function of normalized surface excess. The solid line is limiting dry brush value in each case

adsorption profiles are not strong functions of N_1/N_2 so long as $N_1/N_2 \geq 1$. In terms of the situations discussed by Shull we appear to have weak adsorption for this system because ϕ_B has a finite value. However, this situation is equivalent to a strongly adsorbed brush superimposed on a background equal to ϕ_B; therefore, we anticipate that parameters obtained here, i.e. the brush height z_{off}, surface excess (both normalized by R_{gDPSF}) and the ϕ_s, should be in agreement with the values given by Shull. *Figure 12* compares our values of these parameters as a function of z^*/R_g with the predictions for the limiting dry brush case[17]. Contrary to the expectations based on *Figure 11* the surface volume fraction is in good agreement with the limiting dry brush values. However, the brush height obtained from reflectometry data is *ca* 1.5 times greater than the predictions of SCF theory. This is surprising because strong stretching of the end tethered molecules is only expected when the grafting density (number of chains attached per unit area) is large and the surface is saturated by adsorbing polymer. As *Figure 12a* shows, the data obtained by us are still far from saturation, which is approached when the normalized surface excess approaches a value of 2. The DPSF molecules appear to be only weakly adsorbed at the vacuum surface, which is not saturated by them although the molecules are highly stretched. A possible explanation could be that the system, despite being annealed for two days, is not at equilibrium. The fluorine ends are attracted to the surface and begin to diffuse rapidly to the surface, but the remainder of the molecule has not had sufficient time to relax to an equilibrium configuration which is less extended. If this were a plausible explanation, then both the surface volume fraction of DPSF and the surface excess would change on annealing further. SIMS experiments[22] showed that the change of surface concentration of atoms on annealing these mixtures for times up to five days was negligible. Additionally, our kinetics experiments[40] using NR analysis show that the surface excess reaches an equilibrium value in *ca* 1 h of annealing; furthermore, the brush height (z_{off}) also stabilizes within this time. Moreover, the parameters z_{off} and w would change on annealing; this is not observed.

We have suggested above that the DPSF is only weakly adsorbed at the vacuum surface. Our sticking energy of $1.9k_BT$ should be compared to the value of $8.6k_BT$ obtained by Clarke *et al.*[19] for carboxylic acid terminated deuteriopolystyrene end attached to the silicon substrate, and for the value of *ca* $4.2k_BT$ obtained by Jones *et al.*[8] for silane terminated DPS similarly adsorbed, these comparisons substantiate the weak adsorption suggestion. For predictive purposes it would be useful to calculate a value of β from known parameters using equation (2). Taking $\delta_s = a$, the statistical segments' length for polystyrene and using a value of 6.7 Å with $\beta = 1.9k_BT$ we obtain $(\chi_e^B - \chi_e^s) = 4.0$. An estimate of χ_e^B can be obtained using solubility parameters for polystyrene and polytetrafluoroethylene as a substitute for the perfluorohexyl group:

$$\chi_e^B = \frac{V_L}{k_BT}(\delta_{PS} - \delta_{PTFE})^2 \qquad (7)$$

Values of the solubility parameters, δ_i, were obtained from the literature[41] and the lattice cell volume, V_L, was calculated as a^3. At $T = 400$ K we obtain $\chi_e^b = 3.1$. The term χ_e^s is the surface energy difference per lattice cell between the end perfluorohexyl residue and a styrene segment; it may be expressed as

$$\chi_e^s = \Delta\gamma/n_L k_B T \qquad (8)$$

Where n_L is the number of lattice cells per square metre, and $\Delta\gamma$ is the difference in surface energies of the two components. Literature values[41] for the surface tension of polystyrene extrapolated to 400 K suggest that 32.8 mJ m^{-2} is an acceptable value. For the fluorine end label we have used the surface tension of a short fluorocarbon ($C_{21}F_{44}$), a value of 14.4 mJ m^{-2} being reported[41]. Consequently $|\Delta\gamma| = 18.4$ mJ m^{-2} and $|\chi_e^s| = 1.5$. There is ambiguity about the sign of $\Delta\gamma$ and χ_e^s; since we know that adsorption is favoured by $(\chi_e^b - \chi_e^s)$ being positive, we anticipate the χ_e^s should be negative. On this assumption we obtain $(\chi_e^b - \chi_e^s) = 4.6$, which in view of the approximations inherent in the use of solubility parameters is in excellent agreement with the values from the SCF calculations. Notwithstanding this agreement we stress that this estimation procedure is highly speculative, but may prove a useful method to approximate the sticking energy.

Our earlier X.p.s.[22] experiments indicated that there

was at least twice as much fluorine at the surface than anticipated from the composition. Similarly, Hunt *et al.*[37] have reported the results of an angle dependent X.p.s. analysis of an identical polymer as the DPSF used here except that the polystyrene was hydrogenous. For an X.p.s. sampling depth of 20 Å, they report that the surface fluorine content is *ca* 7.6 times that of the bulk. Recently, Elman *et al.*[42] have used NR to investigate the surface segragation of functional end groups. The low surface energy group they used was identical to the fluorine end label used by us, but the polystyrene was a linear diblock copolymer of *ca* 80 units of HPS followed by 19 units of deuteriostyrene before termination by the fluorosilane. The molecular weight of this polymer was very low at *ca* 10 000 g mol^{-1}. Additionally, since the aims of Elman *et al.*'s work was to gain evidence for a periodical distribution of end groups at the surface, the pure polymer was investigated, i.e. it was not mixed with unlabelled material. Hence, apart from agreeing with our findings here, i.e. that there is an excess of the fluorine ends at the surface, the results obtained cannot be compared to ours.

CONCLUSIONS

We have demonstrated that placing a fluorocarbon unit at one end of a deuteriopolystyrene molecule of low molecular weight is sufficient to cause a surface excess layer of the deuteriopolystyrene to be formed at the vacuum surface on annealing. Values of the surface excess (z^*) obtained by NRA and NR techniques agree with each other, but the resolution of the NRA is much reduced from that of NR. Only the NR had sufficient resolution to provide parameters which characterized the shape of the near surface depth profile. NR data showed that there was formation of a partial surface excess before annealing, but NRA could not detect this. Deuteriopolystyrene without the fluorinated end group was not adsorbed and this fact in conjunction with our earlier X.p.s. and SIMS results leads us to conclude that the end fluorinated polystyrene is tethered by its fluorine end to the vacuum/polymer film interface. The parameters of this deuteriopolystyrene rich region have been compared to the numerical predictions of a SCF theory for polymer brushes. When a sticking energy of 1.9 $k_B T$ is used the values of the surface excess predicted by the theory are well supported by the experimental results. The detailed shape of the experimentally obtained profiles is not reproduced and this appears to be symptomatic of systems where the sticking energy is low. However, the experimental brush height appears to be larger than anticipated for a dry brush where the sticking energy is rather small. Estimates of the sticking energy by an empirical method, using solubility parameters and surface tensions of similar low molecular weight materials, produce a value in very good agreement with that obtained from comparisons between SCF calculations and near surface depth profiles obtained from NR.

ACKNOWLEDGEMENTS

R.W.R. and I.H. thank EPSRC for the support of this research via a co-operative award. The EPSRC are also thanked for the provision of neutron beam facilities at the Rutherford Appleton Laboratory and nuclear reaction analysis facilities at the University of Surrey. R.W.R. and I.H. are particularly grateful to Professor Ken Shull of Northwestern University, Illinois, for providing a copy of his self-consistent field computer program and for discussions of the data presented here.

REFERENCES

1 Adamson, A. W. 'Physical Chemistry of Surfaces', John Wiley, New York, 1990
2 Nakanishi, H. and Pincus, P. *J. Chem. Phys.* 1983, **79**, 997
3 Schmidt, I. and Binder, K. *J. Phys. (Paris)* 1985, **46**, 1631
4 Carmesin, I. and Noolandi, J. *Macromolecules* 1989, **22**, 1689
5 Jones, R. A. L. and Kramer, E. J. *Polymer* 1993, **22**, 115
6 Jones, R. A. L., Kramer, E. J., Rafailovich, M. H., Sokolov, J. and Schwarz, S. A. *Phys. Rev. Lett.* 1989, **62**, 280
7 Jones, R. A. L., Norton, L. H., Kramer, E. J., Composto, R. J., Stein, R. S., Russell, T. P., Mansour, A., Karim, A., Felcher, G. P., Rafailovich, M. H., Sokolov, J., Zhau, X. and Schwarz, S. A. *Europhys. Lett.* 1990, **12**, 41
8 Jones, R. A. L., Norton, L. J., Shull, K. R., Kramer, E. J., Felcher, G. P., Karim, A. and Fetters, L. J. *Macromolecules* 1992, **25**, 2359
9 Hariharan, S. K., Kumar, S. K. and Russell, T. P. *J. Chem. Phys.* 1993, **98**, 4163
10 Cowie, J. M. G., Devlin, B. G. and McEwen, I. J. *Macromolecules* 1993, **26**, 5628
11 Jong, L., Pearce, E. M., Kwei, T. K., Hamilton, W. A., Smith, G. S. and Kwei, G. H. *Macromolecules* 1992, **25**, 6770
12 Bhatia, Q. S., Pan, D. H. and Koberstein, J. T. *Macromolecules* 1988, **21**, 2166
13 Reivilar, M., Bothelo do Rego, A. M., Lopes de Silva, J., Abel, F., Quillet, V., Schott, M., Petitjean, S. and Jerome, R. *Macromolecules* 1994, **27**, 5900
14 Fleer, G. J., Cohen-Stuart, M. A., Scheutjens, J. M. H. M., Cosgrove, T. and Vincent, B. 'Polymers at Interfaces', Chapman and Hall, London, 1993
15 Scheutjens, J. M. H. M. and Fleer, G. J. *J. Phys. Chem.* 1980, **84**, 178
16 Helfand, E. and Wasserman, Z. R. 'Developments in Block Copolymers' (Ed. I. Goodman), Applied Science Publishers, London, 1982
17 Shull, K. R. *J. Chem. Phys.* 1991, **94**, 5723
18 Clarke, C. J., Jones, R. A. L., Edwards, J. L. Shull, K. R. and Penfold, J. *Macromolecules* 1995, **28**, 2042
19 Clarke, C. J., Jones, R. A. L., Edwards, J. L., Clough, A. S. and Penfold, J. *Polymer* 1994, **35**, 4065
20 Nicolai, T., Clarke, C. J., Jones, R. A. L. and Penfold, J. *Colloids and Surfaces A: Phys. Eng. Aspects* 1994, **86**, 155
21 Mansfield, T. R., Iyengar, D. B., Beaucage, G., McCarthy, T. J., Stein, R. S. and Composto, R. J. *Macromolecules* 1995, **28**, 492
22 Affrossman, S., Hartshorn, M., Kiff, F. T., Pethrick, R. A. and Richards, R. W. *Macromolecules* 1994, **27**, 1588
23 Cahn, J. W. *J. Chem. Phys.* 1977, **66**, 3667
24 Russell, T. P. *Mater. Sci. Rep.* 1990, **5**, 171
25 Penfold, J. and Thomas, R. K. *J. Phys. Condens. Matter* 1990, **2**, 1369
26 Richards, R. W. and Penfold, J. *Trends Polym. Sci.* 1994, **2**, 5
27 Stamm, M. in 'Physics of Polymer Surfaces and Interfaces' (Ed. I. Sanchez), Butterworth-Heinemann, Boston, 1992
28 Kunz, K., Reiter, J., Götzelmann, A. and Stamm, M. *Macromolecules* 1993, **26**, 4316
29 Pedersen, J. S. *J. Appl. Cryst.* 1992, **25**, 129
30 Pedersen, J. S. and Hamley, I. W. *Physica B* 1994, **198**, 16
31 Sivia, D. S., Hamilton, W. A. and Smith, G. S. *Physica B* 1991, **173**, 121
32 Press, W. H., Teukolsky, S. A., Vetterling, W. T. and Flannery, B. P. 'Numerical Recipes. The Art of Scientific Computing', Cambridge University Press, Cambridge, UK, 1992
33 Payne, R. S., Clough, A. S., Murphy, P. and Mills, P. J. *Nucl. Instrum. Meth. Phys. Res.* 1989, **B42**, 130

34 Jones, R. A. L. in 'Polymer Surfaces and Interfaces II' (Eds W. J. Feast, H. Munro and R. W. Richards), John Wiley, Chichester, 1993
35 Bates, F. S. and Wignall, G. D. *Phys. Rev. Lett.* 1986, **57**, 1429
36 Richards, R. W. and Thompson, H. L. unpublished results
37 Hunt, M. O. Jr, Belu, A. M., Linton, R. W. and DeSimone, J. M. *Macromolecules* 1993, **26**, 4854
38 Cotton, J. P., Decker, D., Benoit, H., Farnoux, B., Higgins, J. S., Jannink, G., Ober, R., Picot, C. and des Cloizeaux, J. *Macromolecules* 1974, **7**, 863
39 Brandrup, J. and Immergut, E. H. 'Polymer Handbook', 3rd Edn, John Wiley, New York, 1989
40 Hopkinson, I. PhD Thesis, University of Durham, UK, 1994
41 Van Krevelen, D. W. 'Properties of Polymers', 3rd Edn, Elsevier, Amsterdam, 1990
42 Elman, J. F., Johs, B. D., Long, T. E. and Koberstein, J. T. *Macromolecules* 1994, **27**, 5341